Limit analysis discussion of design methods for fracture of timber dowel joints loaded perpendicular to grain

T. A. C. M. van der Put

Faculty of Civil Engineering and Geosciences, Timber Structures and wood technology, TU Delft, P.O. Box 5048, 2600 GA Delft The Netherlands

ABSTRACT:

The results of an investigation of splitting of joints of [1] are used for a discussion of design methods and as necessary answer on comments and for confirmation of the extended fracture mechanics theory which accounts for the part of the external energy which is needed for plastic dissipation at the dowels, (which cause the crack opening). It is shown that exact theory always is needed to give a precise description of fracture behavior for a real calculable reliability in all circumstances. It further is shown that applied cohesive zone models, J-integral, and finite element solutions, are questionable and always need to be explained and controlled by theory. Important is, that these empirical fitting procedures are not able to fit to any relation, as follows from exclusion by the "lack of fit" test. Contrarily, limit analysis theory shows a precise fit (with a coefficient of variation of 10%) to the theory equation and delivers a conclusive confirmation of criticized design rules of Eurocode 5.

KEYWORDS: *wood, limit analysis, fracture mechanics, cohesive zone model, J-integral, finite element method, splitting of timber pin-dowel connections.*

I.   INTRODUCTION

Exact theory represents the law of nature and controls the rightness of empirical data. It provides the only possibility of the, by European law demanded, sufficient, calculable, reliability, even for never measured cases. The contrary empirical approach of the data of [1], (an investigation on splitting of joints), is discussed to show the general validity of exact theory and to analyze proposed, untenable, design rules. This exact limit analysis approach was developed in [2] as reaction on the inadequate, empirical curve fitting method of [3]. The design method of [2] was applied since 1990 in Eurocode 5 and therefore followed by several countries as e.g. by the Dutch Timber Code. By the definition of a limited ultimate deformation of dowels as design requirement, separate rules were possible for splitting of the beam and for the bearing capacity of the dowels of the joint. Later this limited deformation rule for the dowel strength was abandoned for these type of joints and solely splitting was chosen as end state for the strength. Thus failure may be rather sudden by splitting of the beam, or by splitting after early flow of the dowels after a long hardening stage, (which is possible by hardening due to confined dilatation of the embedment stress). The possibility of brittle failure was corrected in 2000, by limiting the ultimate dowel loading below the lowest splitting boundary of the beam. "Flow" of the dowel then is always determining for the strength of the joint, as was the case before. A precise description by theory of all new published data, every ten years, was given in [2] and [4], and here for the last new data of [1]. There nevertheless remain misinterpretations of data and theory. The error mostly made, by comparisons, is, that the lower boundary design equation of the Eurocode (reduction factor 0.67), which always prevents splitting and provides that dowel failure is always determining, is regarded as the mean strength equation. Further, the factor $\sqrt{n/n_g}$ of eqs.(B.5 or B.6) is left out, showing that never these real mean strength equations, are regarded at comparisons and also is not known when and why the minimum value of $\sqrt{n/n_g} = 0.67$ applies. Because design is chosen in CIB-W18 to provide a safety against the lowest splitting force, by choosing the dowels to be always determining for failure, the impression is given of an underestimation of the strength by this factor 0.67. In the following is shown, that the tremendous random spreading of outcome of the applied methods of [1], (given in [5]), have to be replaced by exact theory to show a precise data fit (here with a coefficient of variation of 10%), as to be expected, and as applies for all thus far published data on this subject. A right conclusion thus should not concern the exact theory (as always done) but only may confirm that the empirical data, the measurements, can be trusted (which thus is shown here to be the case for data of [1]). In the following, first the applied methods of e.g. [1], given in [5] and [6], have to be discussed.

II.   DISCUSSION OF APPLIED CALCULATION METHODS

2.1. Discussion of Cohesive zone models

Nearly all assumptions of the cohesive zone models are against exact theory. The most fundamental violence is to regard the stress of the softening curve, which is a nominal stress, representing the unloading of the specimen due to crack extension, thus is the stress far <u>outside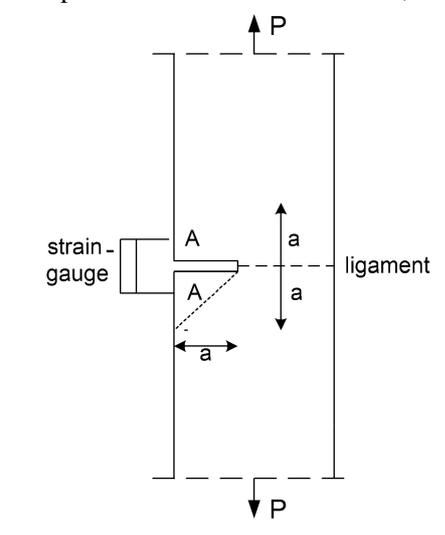</u> the fracture plane, (the stress ad infinitum), to be the stress <u>in the fracture plane</u> (the ligament), while the real mean stress in that plane is ultimate, thus constant, (but may show some hardening at the start instead of softening). The derivation of the softening curve of the center notched specimen is given in [7], Section 3.3. The curve represents the decrease of ultimate loading and of the stiffness, due to crack extension in the specimen and shows a constant energy release rate at every point of the softening curve, <u>thus a constant fracture energy</u> and is therefore called Griffith locus. The derivation shows that there is no need for contradictions as negative stiffness and negative dissipation. This also follows from molecular deformation kinetics, [8], showing a common primary bond breaking process in the ultimate stress zone. For the dowel connection this derivation is given in the Appendix. For instance for the constant strain rate test, also β of eq.(B5), increases linearly with time, and for long cracks, the softening follows $V_f \approx C_1 / a$.

Thus there is a constant ultimate moment: $M_u \approx V_f \cdot a = C_1$ and V_f has to diminish at the increase of a. There thus is no diminishing strength, but unloading of the specimen. Eq.(B6) shows that, at the start of crack extension, which represents the ultimate state, the ultimate value of V_f is constant (by shear failure, according to the critical distortional energy criterion [14] as highest lower bound solution).

The aim of the cohesive zone model was to remove infinite tensile stresses of the singularity method, by substitution of an internal compressional equilibrium system which neutralizes the singularity. However, this superposition of closing stresses is superfluous because the singularity does not exist and the singularity solution, or mathematical flat crack solution, also is an single mode approximation, which is not applicable for the always occurring combined loading modes. The singularity is an empty space within the crack boundaries and there thus is no material which can be stressed infinitely high. The crack problem thus restricts to the boundary of the crack, thus is a common limit analysis boundary value problem at the crack boundary, or better, at the elastic-plastic boundary of the plastic and fractured zone around the crack and crack tip. All kinds of dissipation within this boundary determines the fracture energy (= energy release rate). The exact solution of the Airy stress function is given in e.g.[7] and shows that fracture of clear wood always occurs, for any load combination, by reaching the uniaxial ultimate tensile stress (cohesion strength) at the crack boundary near the crack tip, what leads to the parabolic Wu-mixed mode failure criterion: $K_I / K_{Ic} + \left(K_{II} / K_{IIc} \right)^2 = 1$ (1)

Eq.(1) thus is the exact criterion, in accordance with the measurements of precise tests (of e.g. [9] and [10]). By this solution (in [7]), the real "traction stresses" in the fracture plane are known. However the cohesive zone model assumes the existence of a crack opening law, by measuring the displacement over the crack opening as given in Fig. 1. The total applied external work on the specimen, however, follows from load, and the displacement of that load at the specimen. The load at crack extension is about proportional to the remaining ligament length for long cracks, because of the constant mean ultimate stress in the ligament (for high loaded ligament in the end state). Thus, to maintain equilibrium the external force diminishes in proportion to the remaining ligament decrease. The deformation increases because of the decrease of the stiffness of the specimen by crack extension. Yield drop necessarily occurs because the rate of fracture is much higher than the rate of straining by the constant strain rate test. <u>Measuring deformation over a crack opening has no meaning</u> because it is not known what is measured. In Fig. 1, the stress and strain at the points A are zero, due to the unloaded triangles adjacent to the crack, and the crack opening will be proportional to the crack length a by this local unloading, and is not related to the constant ultimate stress in the remaining intact ligament. The area under the non-linear part of the real load – displacement curve determines the total applied external work on the specimen. Half of this area is the elastic strain increase and the other half is the fracture energy (= equal to the elastic energy increase). The cohesive zone model regards the total area, thus the total external energy as fracture energy, thus more than <u>a factor 2 too high</u>. Further is this energy wrongly related to the area of the crack length increase instead of to the total crack length area, including the initial crack length. <u>By doing so, the fracture energy per unit area (which should be equal to the energy release rate) is not a material constant but depends on</u>

Fig.1. Nonsence data

(labels on figure: P, strain-gauge, A, A, a, a, a, ligament, P)

the chosen initial crack length. Further, the total measured energy has to be divided among the different acting processes. The deformation kinetics activation energy and concentration tells whether the primary bond breaking process of fracture is dominating in the test. The cohesive zone model does not account for this result of the exact theory of molecular deformation kinetics, (see [8]). This kinetics theory also explains why softening only is possible in a constant strain rate test and is not possible in a constant loading rate test and in a dead load test to failure. Because in practice only dead load failure occurs, is it astonishing that impossible softening then is regarded as a constitutive traction law. A severe lack of distinction of acting kinetic flow processes is made by the cohesive zone model of dowel connections in wood. Most of the energy obtained from the area of the load-displacement curve is <u>not by tensile traction</u> <u>but due to compressive</u> dowel embedment <u>hardening</u>, showing clearly that this area method of the load-displacement curve is not able to give the real fracture energy and thus never should be applied. Most investigations on connections are with one- or a few dowels, where the dowel is determining for initial "flow" [4]. This applies especially for the in practice applied slender dowels, thus up to connections with 9 to 12 nails. Then the dowel is determining for the ultimate load and not splitting of the beam, which occurs after flow and hardening of the embedment, because the dowel performs a crack opening movement at embedment failure. The exact derivation, as boundary value solution, based on the shear-line (called slip-line) construction, of the embedding strength is given in [11], with the simplification to the simple spreading model. It is shown below that this spreading model has to be applied on the relevant data of [1]. In the 2D cohesive zone model for dowel-connections, the measured triaxial <u>compressional</u> hardening is regarded to be a <u>tensional</u> hardening of traction, leading to random results, with an extreme high variability, and a statistical exclusion of fit to any equation. The reason of this mismatch lies in the method itself because nearly all model assumptions are strongly against exact theory and generally against thermodynamics and even the tensile strength is not ultimate but variable down to zero (called cohesive forces). It is shown in Section 2.3 that strain hardening, in stead of strain softening, exists in the critical section.

2.2. The questionable application of the *J*-integral

The *J* integral, around a crack tip, applies for a (nonlinear) elastic material and only then *J* has the meaning of an energy-release rate G_c. The theory is valid for radial monotonic loading and precludes unloading and is then, mathematically equivalent to a nonlinear theory of elasticity. The influence of the behavior of wood according to the flow theory of plasticity prevents, even under monotonic loading, that the path-independence of *J* can be established. Under the applied loading histories of [1], after blunting of the top of the loading curve, (which includes loading and unloading), *J* is not only not path-independent, but also has no physical meaning. Thus the formation of the fracture process zones, and of flow, during crack growth means non-proportional plastic deformation which invalidates the deformation theory of plasticity. Instead limit analysis applies as e.g. shown here by its precise data fit. According to limit analysis, it is possible to replace the first rising elastic-plastic loading curve by a non-linear elastic curve as a lower bound solution. However crack extension start at the top of the loading curve and the full value of G_c is reached over the top of the curve at the start of unloading. Thus the replaced rising curve is before the top, outside the crack extension and process zone dissipation and will not give a right value of G_c. Thus, the validity of *J* has to be denied and the thereupon based fracture energy plots, (after partial unloading) as given by Figures 13 to 16 of [6], thus have no meaning. By that, also the found differences of mode I and II critical fracture energies, with respect to the usual values for wood, are probably explained. Although it is supposed in [1] that this difference is caused by the different stress situation with respect to the standard tests, this cannot be true. The by the J-integral, or by crack closure technique or compliance method obtained critical energy release rate (or fracture energy) is independent of the type and form of the specimen and is equal for all tests for initial fracture. That is why the geometrical form factor of a specimen type can be estimated empirically. Thus the application of the J-integral always should have been controlled e.g. by the compliance method. A compliance variation could have been simulated by the applied computer model by measuring the deflection at the loading points, at varying crack length a, at constant load, giving the constants B_1 for the compliance: $C = B_0 + B_1 a + B_2 a^2 + B_3 a^3 + ...$ and the energy

release rate: $G_t = \left(F^2 / 2b \right) \cdot \left(\partial C / \partial a \right) = \left(F^2 / 2b \right) \cdot \left(B_1 + 2B_2 a + 3B_3 a^2 \right)$ (2)

where *b* is the beam width and G_t will be about equal to the real mode I fracture energy. Of course it is easier and better to apply the exact eq.(B.6), based on the calculated compliance difference, as shown in the Appendix.

2.3. Softening and hardening behavior

It is accepted in [1] that the finite element method is not able to show and explain real behavior, but only is able to give an imitation of such behavior. For instance embedment flow and hardening by confined dilatation is imitated by using a bilinear straining diagram, which imitates a flow point and hardening slope at loading which next is accounted as hardening of the fracture energy, leading to non-existent, nowhere else found, crack

resistance curves. The same applies for softening. The impossible assumption of linear softening behavior, given by Fig.2 of [6], as physical material property, for the so called cohesive zone material, is not right and leads to models with negative spring constants and allows construction of perpetuum mobile. The apparent softening is due to unloading of the specimen, outside the high loaded fracture plane. The stress in the fracture plane initially increases at crack extension because the intact zone of the fracture plane decreases. The Griffith stress of e.g. the center notched specimen of Fig. 2 is $\sigma_g = \sqrt{G_c E / \pi a}$, which is a nominal stress, thus is the stress in the intact elastic material outside the fracture plane, and is not the failu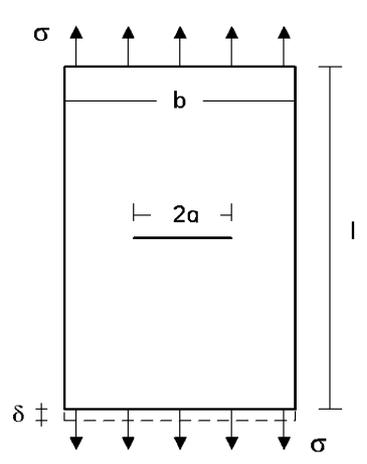re stress. The real mean stress σ_w in the fracture plane is a factor $b / (b - 2a)$ higher according to Fig. 2 and is $\sigma_w = \left(\sqrt{G\,E / \pi a} \right) / (1 - 2a / b)$ and thus is an increasing stress with crack extension and crack opening increase. It is thus necessary to speak of hardening because the stress in the critical section initially increases at crack extension: Thus the real critical stress in the critical fracture section increases by crack extension when:

$$\frac{\partial \sigma_w}{\partial (a/b)} = \sqrt{\frac{G_c E}{\pi b}} \cdot \frac{-1 + 6a/b}{2(a/b)^{1.5}(1 - 2a/b)} > 0 \tag{3}$$

σ

b

⊢ 2a ⊣

l

δ ‡

σ

Fig.2 Center notched specimen

Thus when $a/b > 1/6$. The lowest value of [7]:

$a_c / b = \sqrt{l / 6\pi b} \geq 1/6$ when $l/b \geq 0.5$. Thus when the length l of the specimen is higher than 0.5 times the width *b*. This always applies because for $l/b < 0.5$, the two crack tips act independently of each other. The increase, p.e. of the "traction stress" at increase by a factor 2 of the crack length occurs when:

$$\frac{\sigma_{w1}}{\sigma_{w2}} = \frac{\sqrt{G_c E / \pi a} / (1 - 2a/b)}{\sqrt{G_c E / \pi 2a}(1 - 4a/b)} < 1 \tag{4}$$

Thus when $\sqrt{2}(1 - 4a/b) < (1 - 2a/b)$ or: $a/b > 0.113$. This applies because $a/b > 1/6$. Thus the decreasing fracture plane is always in the ultimate state and the external load has to diminish to maintain equilibrium. It thus is necessary to apply real ultimate failure conditions, based on the known molecular deformation kinetics processes [8] and on fracture mechanics (see Appendix).

For wood, tested on a stiff specimen in a stiff testing rig [12], the, near at the top blunted loading curve, shows enough plasticity for a total stress redistribution and the value of the energy release rate or fracture energy, which is of higher order than the energy needed for separation of the material, shows explicitly the large amount of plastic flow which accompanies and explains crack growth (and small crack formation in the fracture zone) [13], [7]. The right approach thus is the linear elastic-full plastic approach of limit analysis, what explains the possibility of many exact solutions (of the Airy stress function) differing an internal equilibrium system from each other and from the real occurring solution [7].

2.4. Applied failure criterion

The in [1] proposed failure criterion, eq.(1) of [1] does not meet the prescribed ductile failure state by embedment flow, as also was prescribed in the past in all regulations. To avoid splitting in all circumstances, the dowel connection has to be designed for maximal 0.67 times the maximal splitting force of the beam, as is still prescribed in the Eurocode 5.

The validity of eq.(2) of [1], has to be shown. Only a theoretical right equation may provide real calculable reliability and safety. An empirical equation is not identical to the exact equation and thus is unsafe and wrong in other, and in general applications.

Inserting eq.(3) in eq.(2) of [1], and using eq.(7), gives:

$$\frac{G_{spec}^I}{G_c^I} + \frac{G_{spec}^{II}}{G_c^{II}} = k_r = 1 \quad \text{or:} \quad \frac{K_{I,spec}^2}{K_{I,c}^2} + \frac{K_{II,spec}^2}{K_{II,c}^2} = k_r = 1 \ . \tag{5}$$

According to eq.(5.4) of [7], Section 5.2, this is a right theoretical equation according to the orthotropic critical distortional energy principle of [14], of the start of initial elastic distortional energy dissipation. However, the equation only applies for orthotropic materials with equal compression and tension strengths, thus not for wood. Outer this theoretical exclusion, there is an empirical exclusion by a lack of fit as follows from the last equation of Table 1. The same applies for the in [1] referred results of M.H. Kasim, who uses the second

Table 1. - Lack of fit values for different failure criteria [10]

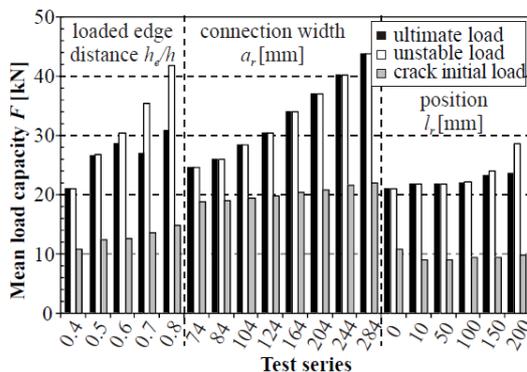| Failure criterion	p-value
$K_I / K_{Ic} = 1$	0.0001
$K_I / K_{Ic} + K_{II} / K_{IIc} = 1$	0.0001
$K_I / K_{Ic} + \left(K_{II} / K_{IIc} \right)^2 = 1$	0.5629
$\left(K_I / K_{Ic} \right)^2 + K_{II} / K_{IIc} = 1$	0.0784
$\left(K_I / K_{Ic} \right)^2 + \left(K_{II} / K_{IIc} \right)^2 = 1$	0.0001
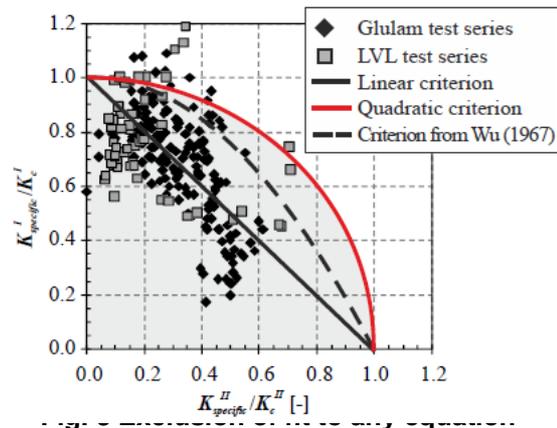
Fig. 3. Exclusion of fit to any equation

equation of Table 1. Both equations are strongly excluded by lack of fit at the, for wood, common variability. It has to be explained why the exact failure criterion (the third equation of Table 1) is excluded in [1]. The exact derivation of this parabolic Wu-equation is given in e.g. [7]. This is verified by precise measurements of [9]. This also is verified by tests of [10] done at the TL-system on eastern red spruce at normal climate conditions using different kinds of test specimens. The usual finite element simulations provided the geometric correction factors, and the stress intensity factors. The lack of fit test was performed on these data, at the for wood usual variability, assuming the five different failure equations of Table 1. The statistical lack of fit values in the table show, that only the Wu-failure criterion cannot be rejected due to lack of fit. The Wu-equation is shown to fit also clear wood strength data in [14] and [15], as expected from theory. Because the variability of the data of [1], indicated by Fig. 3, (Fig. 8 of [1]), is much higher than those of specialized investigations of [9] and [10], it is clear that the lack of fit exclusion to any equation will apply for the data of [1].

III.   DISCUSSION AND EXPLANATION OF THE GLULAM TEST RESULTS OF [1]

The Glulam test results, which are the basis of the proposed design rules in [1] are given below as graphs: Fig. 4 and 5, (after Fig. 8 and 9 of [6]), following from a loaded dowel connection in a three point bending test (see Fig. 1 of [5]). It was shown in [2], that for connections with 1 or 2 dowels, dowel failure, and not splitting, is the primary failure cause. Splitting occurs after proceeded plastic dowel deformation with hardening. Thus design rules against splitting should not be based on the data of Fig. 4, wherefore dowel embedment failure is determining for connections with less than 3 dowels $(n_c / 2 < 3)$. Also the application of a single dowel in force direction is not right, because of the indeterminacy of the reaction force of the eccentric dowel-force. Further the slenderness $b/d = 80/20 = 4$ (or $63/20 = 3$ for LVL) is too low. The application of these joints thus is not allowed and should not have been accounted as basis of design rules and certainly not for splitting.

3.1. Discussion of triaxial compressional dowel embedment failure, Fig. 4.

In Fig. 4, (which is Fig. 8 of [6], used in [1]), the Glulam data of the investigation of one- and two dowel connections are given. The dimensions of the beam are denoted by $b/h/L$ and h_e is the upper dowel distance to the lower beam edge. Because these connections are not allowed in practice, and by compressional dowel failure, don't give information on initial fracture mechanics, only the measured strength characteristics are explained here in the following. The left column of Fig. 4, giving the influence of h_e / h of the one dowel connections, shows that after sufficient plastic deformation (wherefore the black lines apply), a local failure mechanism around the dowel is determining when $h_e / h \geq 0.5$, giving a load

Fig. 4. Load capacities 1 and 2 dowel joints

capacity of about 28 kN. The strength at $h_e / h = 0.4$ is clearly lower, because now the reduced spreading strength of the dowel is determining [10]. Based on these data, is $h_e / h \approx 0.6$ the boundary of equal strength by the local failure mechanism around the dowel and the spreading strength. Based on this spreading strength then

is for $h_e / h = 0.4$, the strength: $\left(\sqrt{0.4 / 0.6}\right) \cdot 28 = 22.8$ kN, close to what is measured. The dowels of the right column of Fig. 4, are the same as this dowel, with the same spreading possibility and thus are as strong and thus independent of the location (as measured).

For the 2-dowel connections of the middle column of Fig. 4, is also the spreading possibility determining for the initial strength (because $h_e / h = 0.4$), wherefore now the part Fig. 4. Load capacities for 1 and 2 dowel joints between the 2 dowels is determining. Thus, the highest strength of about 44 kN occurs at a dowel distance of 284 mm. Then the strengths for the other distances are:

Dowel distance (mm)	X =	284	244	204	164	124	104	84	74
Strength $\sqrt{(X / 284)} \cdot 44$ kN	=	44	41	37	33	29	27	24	22

as is measured.
Herewith the data of Fig. 4 are explained by initial plastic flow of the dowel embedment.

3.2 Discussion of data of multiple dowel joints of Fig. 5 (Fig. 9 of [6]).

The dimensions of the tested beams were: b/h/L = 80/304/1320 mm; $h_e / h = 0.7$; $a_r = 320$ mm ($a_r =$ width of the dowel pattern). The third column of Fig. 5 (Fig. 9 of [6]) shows that the joints with 6, 9 and 12 dowels are about equally strong with a load capacity of about 95 kN. The left column predicts that n_c in $\sqrt{n / n_c}$ is about 5.5, because then the load capacity is $\sqrt{4 / 5.5} \cdot 95 = 81$ kN for the 4 dowel joint and then: $0.67 \cdot 95 = 63$ kN, for the 2 dowel joint, as measured. Because 2 dowels are less than $5.5 \cdot 0.45 = 2.5$, the minimum value of 0.67 applies (see Appendix).
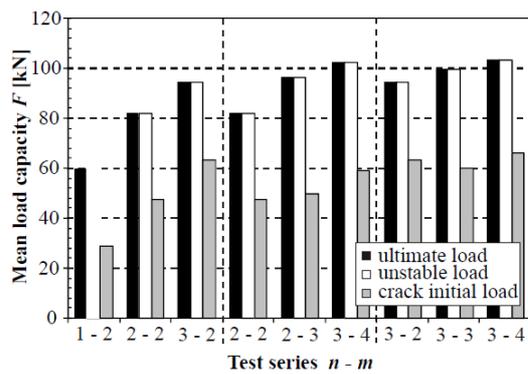

Fig. 5. Load capacity for multiple dowel joints

This splitting independent on the number of dowels, here 6, 9 or 12 dowels, is discussed before in [4], where also the minimal factor of 0.67 is measured for all different types of joints of [3]. Table 7.1 of [4] shows e.g. for series B, that splitting of the beam is determining, showing the same strength, whether there are 10, 15, 20 or 25 nails per shear plane.

The fracture theory, discussed in the Appendix, is thus precisely followed and therefore confirmed by the multi dowel data of Fig. 5. According to eq.(B.6) is $\sqrt{G G_c} = 17.3 N m m^{-1.5}$, which is comparable with the de value of 18 $N m m^{-1,5}$ of [4]. As lower boundary value, of he lowest possible splitting force, is the value:

$0.67 \sqrt{G G_c / 0.6} = 15.5 N m m^{-1.5}$ since 2000 applied in e.g. Eurocode 5 and the Dutch TGB

IV. DISCUSSION AND EXPLANATION OF THE LVL DATA OF [1]

Control and explanation of the data follows e.g. by [7]; eq.(B.5) of' the Appendix. For $a_r = 16d$ in Table 1 below, is the term with β in eq.(B.5) twice the value as for $a_r = 8d$ and because of the quadrat of β is that term 4 times as high. Nevertheless the C- values in the table are hardly higher then, showing the term with β can be neglected and therefore, eq.(B.6) of [7], is applied instead of eq.(B.5), what is right according to limit design to obtain the highest lower bound solution which is equal to the real strength value.

$$V_f = b \alpha h \sqrt{\frac{G G_c / h}{0.6 (1 - \alpha) \alpha + 1.5 \beta^2 G / (\alpha E)}} \cdot \sqrt{\frac{n}{n_c}} \tag{B.5}$$

$$\frac{V_f}{b \alpha h} = \frac{\sqrt{G G_c / h}}{\sqrt{0.6 \cdot (1 - \alpha) \cdot \alpha}} \cdot \sqrt{\frac{n}{n_c}} \tag{B.6}$$

Because flow of the dowel causes crack opening, the factor $\sqrt{n / n_c}$ is needed to account for this combined plastic and elastic dissipation as is derived in [7], at the end of Section 7.2 and given in the Appendix. Eq. (B.6) can be written as a constant *C*, which is the same for all specimens in Table 1-2:

$C = 2 b \cdot \sqrt{G G_c / 0.6} = F \cdot \sqrt{n_c / n} \cdot \sqrt{1 / \alpha - 1} / \sqrt{h}$,

with: $V_f = F / 2$ and: $n_c / n = 1$ when $n \geq n_c$ and $n / n_c = 0.5$, when $n \leq 0.5 n_c$, as is derived. *C* is calculated

(using the data of [5] in column 4) and is given in the last column of Table 1 for the different values of h and $\alpha = h_e / h$ and has the mean value of:

$$C = 2b\sqrt{GG_c / 0.6} = 4.536 \text{ , giving: } \sqrt{GG_c} = \sqrt{0.6} \cdot 4536 / (2 \cdot 63) = 27.9 \, \text{N mm}^{-1.5}$$

This is higher than the value for solid wood and glulam of [2] of 20 $\text{N mm}^{-1.5}$.

Table 1. Test program and results of [5].

Series	Size of specimens $b/h/l$ [mm]	Number of specimens [-]	Dowel strength [kN]	diam. d [mm]	Connection Layout m x n [-]	Edge distance h_e/h [-]	width a_r [mm]	Connection height a_c [mm]	C-factor c kN/mm$^{1/2}$
1	63/400/1600	5	31.5	20	3 x 1	0.20	8d	-	4,45
2	63/400/1600	5	58.6	20	3 x 1	0.40	8d	-	5.08
3	63/400/1600	5	85.1	20	3 x 1	0.60	8d	-	4.91
4	63/400/1600	5	59.7	20	3 x 2	0.40	8d	4d	3.66
5	63/400/1600	5	101.	20	3 x 2	0.60	8d	4d	4.12
6	63/400/2400	5	68.7	20	3 x 2	0.40	8d	4d	4.21
7	63/400/1600	5	76.0	20	3 x 2	0.40	16d	4d	4.65
8	63/600/2400	5	32.8	20	3 x 1	0.13	8d	-	4.89
9	63/600/2400	5	78.1	20	3 x 1	0.40	8d	-	5.53
10	63/600/2400	5	92.0	20	3 x 1	0.60	8d	-	4.34
11	63/600/2400	5	84.1	20	3 x 2	0.40	8d	4d	4.21
12	63/600/2400	5	87.7	20	3 x 2	0.60	16d	4d	4.39
13	63/600/2400	5	90.7	20	5 x 2	0.40	16d	4d	4.53

The mean value of C is 4.536 with a coefficient of variation of 0.1.

The factor: $\sqrt{n_c / n} = \sqrt{6 / n} \le \sqrt{2} = 1.41$, when $n \le 3$, and: $\sqrt{n_c / n} = 1$, when $n \ge 6$.

This means here that this factor $\sqrt{n_c / n} = 1.0$, except for the 3-dowel joints where it is: 1.41.

The data suggest at first glance that $n_c = 6$. A precise value can be calculated by iteration.

V. CONCLUSIONS

- The theoretical equation is shown to fit to the given numerical data precisely (with a coefficient of variation of 10%). This provides a confirmation of the design rules of the Eurocode and provides, as exact theory, the only possible, real, calculable reliability (safety) in all known and new, unknown and unforeseen circumstances.
- The finite element method of [1], [5] is not able to show real behavior, as e.g. embedment flow and hardening and stress spreading effect by confined dilatation and the right unloading behavior. This explains the exclusion of results by the lack of fit to any equation.
- The J integral has no physical meaning by the way it is applied. This may explain the in [1], [5] obtained wrong values of the fracture energies.
- The chosen failure criterion of [1], [5] and [6] applies for orthotropic materials with equal compression and tension strengths, thus not for wood. The criterion also is excluded empirically by the statistical lack of fit test (even for the low variability of the standard fracture toughness tests).
- The theory equations and data show that the influence of a_r can be neglected. There also is no better fit of the data when it is accounted by applying eq.(B.5) instead of eq.(B.6). This means that eq.(B.6) represents the highest lower bound, equal to the real strength.
- It has to be explained why the exact failure criterion (the third equation of Table 1, the only one not excluded by lack of fit) is not applied in [1]. The exact derivation of this parabolic Wu-equation is given in [7], and is verified by advanced research of [9] and [10].
- The investigated brittle joints are not allowed and should not be the basis of empirical rules
- As known, connections with 1 or 2 dowels, show initial dowel failure and not splitting as primary failure cause. Splitting occurs after proceeded plastic deformation and hardening of the dowels. Thus design rules against initial splitting should not be based on these data of dowel embedment failure (as is done).

- One-dowel connections, show, that after sufficient plastic deformation, a local failure mechanism around the dowel is determining when $h_e / h \geq 0.6$. Below this value, the reduced spreading possibility, thus reduced spreading strength, of the dowel is determining.
- For the applied 2-dowel connections, also the spreading possibility is determining (because $h_e / h = 0.4$), wherefore the distance between the 2 dowels is determining for the spreading possibility as follows from theory.
- Because flow of the dowel causes crack opening, the factor $\sqrt{n / n_c}$ is needed to account for this combined plastic and elastic dissipation as shown in [7] and in the Appendix.
- This splitting, independent on the number of dowels, here 6, 9 or 12 dowels, is discussed before in [4], where also the minimal factor of 0.67 is measured for all different types of joints of [3].
- According to eq.(B.6) is $\sqrt{G G_c} = 17.3 \, Nmm^{-1.5}$, for glulam of [1], which is comparable with the de value of 18 $Nmm^{-1.5}$ of [4]. As lower boundary value, based on the theoretical lowest value, $\sqrt{G G_c} = 12 \, Nmm^{-1.5}$ is proposed and applied in e.g. the Eurocode 5 and the Dutch TGB Code during decades.
- Softening as material property does not exist and leads to nonsense models with e.g. negative spring constants. The real stress on the still intact material of the fracture plane increases, or is in the final ultimate state.
  - The increased bearing capacity due to hardening of the dowel embedment strength is wrongly interpreted as an increased tensional fracture resistance. This leads to fictive fracture energies given in the figures of [1].
- The lack of fit test excludes the possibility to base design rules on the results of [1] and [5].
- It was shown 24 years ago by [2] that the exact approach could explain all investigations and could predict never before measured behavior. Ten years later in [4], the same was shown for the investigations during that time. Again, 14 years later, it is here shown that still the exact theory gives the only right explanation. By not following the theory there was a tremendous spill of capital and research capacity by many institutes, by doing superfluous, resultless research, not linked to previous developments and investigations. As long as exact theory is not followed and developed further, there is no progress possible.

References

[1]   Design approach for the splitting failure of dowel-type connections loaded perpendicular to grain, B. Franke, P Quenneville, CIB-W18/46-7-6, meeting 46, Vancouver, Canada, 2013.

[2]   Tension perpendicular to the grain at notches and joints, T.A.C.M. van der Put, CIB-W18A/23-10-1, meeting 23, Lisbon, Portugal, 1990.

[3].   Determination of perpendicular to grain tensile stresses in joints with dowel-type fasteners, Ehlbeck J, Görlacher R, Werner H., CIB-W18, paper 22-7-2, Germany 1989.

[4]   Evaluation of perpendicular to the grain failure of beams, caused by concentrated loads of joints, T.A.C.M. van der Put, A.J.M. Leijten, CIB-W18A/33-7-7, meeting 33, Delft, The Netherlands, August 2000.

[5]   Analysis of the failure behavior of multiple dowel-type connections loaded perpendicular to the grain in LVL, S. Franke, B. Franke, P. Quenneville, World Conference on Timber Engineering Auckland, New Zealand 2012.

[6]   Analysis of the failure behavior of transversely loaded dowel-type connections in wood, Bettina Franke, Pierre Quenneville, World Conference on Timber Engineering, Trentino Italy 2010.

[7]   A new fracture mechanics theory of wood", van der Put T.A.C.M., Nova Science Publishers, New York, 2011.

[8]   Deformation and damage processes in wood, van der Put T.A.C.M., Delft University Press, The Netherlands, (1989).

[9]   Application of fracture mechanics to anisotropic plates, Wu E.M., J Appl Mech 34, 1967: 967–974.

[10]   Criterion for Mixed Mode Fracture in Wood, Mall S., Murphy J.F., Shottafer J.E., J. Eng. Mech. 109(3) 680-690, June 1983.

[11]   Derivation of the bearing strength perpendicular to the grain of locally loaded timber blocks, van der Put T.A.C.M. Holz Roh Werkst, 66 (2008) 409-417.

[12]   Method for determination of the softening behavior of wood etc. Boström L.,Thesis, Report TVBM-1012, Lund, Sweden, (1992).

[13]   Softening behavior and correction of the fracture energy, van der Put T.A.C.M., Theoretical and Applied Fracture Mechanics vol. 48 issue 2 October, 2007. p. 127-139.

[14]   A continuum failure criterion applicable to wood, van der Put T.A.C.M., J Wood Sci (2009) 55:315–322.

[15]   A general failure criterion for wood, van der Put T.A.C.M. Proceed. 15th CIB-IUFRO Timber Eng. Group Meeting, Boras, 1982, Sweden.

VI.   Appendix Energy approach for fracture of joists, loaded perpendicular to grain [7]

The following derivation is given before in different forms, e.g. in [2], [4] and [7], but is not generally known and is therefore in essence repeated here for completeness. The apparent brittle failure of the fracture mechanics tests is due to instability by too low stiffness of specimen and testing equipment. The testing in [12], at sufficient stiffness to follow the theoretical softening curve, shows sufficient plasticity near and at the rounded top for total stress redistribution. This means that limit analysis has to be applied for the ultimate strength analysis providing always possible exact solutions. Because for small deformations, the ultimate limit value, is

not dependent on the followed loading path, the analysis can be based on an elastic-full plastic schematization of the loading curve. This means that in stress space, the flow criterion is a single curve and for "plastic" dissipation, the stress increment vector should be along (tangential to) the concave curve, and the strain vector should be perpendicular to the stress (normality rule) what means that the (maximum) extremum variational principle applies for "flow" and thus the virtual work equations apply and thus the theorems of limit analysis, with the lower and upper bound solutions, applying for any allowable equilibrium system, (e.g. following as solution of the Airy-Stress function). In these small, virtual first order calculations the strength is, except the independence of the loading path, also not dependent on initial stress and internal equilibrium systems. It therefore is appropriate to apply common beam theory, as small, first order expanded behavior, which can be regarded to differ an internal equilibrium system from any real stress state. This also can be stated as follows: Because an internal equilibrium system has no influence on the ultimate strength, the differences of the potential energy of the internal equilibrium systems, of the cracked, and the un-cracked, intact state, should not be accounted and only the first order term has to be regarded. Also lower order effects, as clamping action and lower order bending terms have to be omitted for the highest lower bound solution. Thus the beam theory has to be applied for the right solution (and thus forget the upper bound finite element calculation). This is applied here for the tested beams of [1], thus for a connection at the middle of a beam, to find the compliance difference between the cracked and intact state as follows (see Fig. B.1):

The part above the crack (stiffness $I_2 = b(1-\alpha)^3 h^3 / 12$) carries a moment M_3 and normal force N and the part below the crack (stiffness $I_1 = b\alpha^3 h^3 / 12$) carries a moment M_1, normal force N and a shear force V. and at the end of the crack a negative moment of about: $M_2 \approx -M_1$. Further is $M_2 = M_1 - V\lambda$, thus $M_1 = V\lambda / 2$.
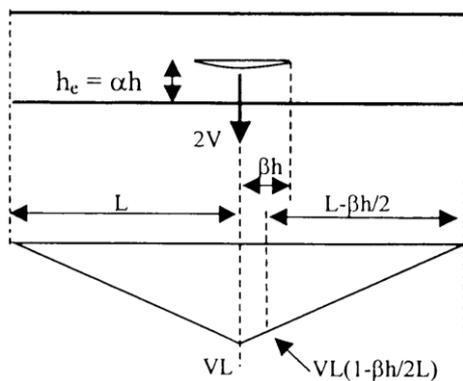
The deformation of beam 2 of the cracked part βh is equal to the un-cracked deformation δ_{un} of that part and the deformation of beam 1 is δ_{un} plus the crack opening δ (see Figures B.1 and B.2) and δ is:

$$\delta = \frac{1}{2} \cdot \frac{V\lambda^2}{EI_1} \cdot \frac{2}{3} \cdot \lambda - \frac{1}{2} \frac{M_1\lambda^2}{EI_1} = \frac{1}{3} \frac{V\lambda^3}{EI_1} - \frac{1}{4} \cdot \frac{V\lambda^3}{EI_1} =$$

$$= \frac{1}{12} \cdot \frac{V\lambda^3}{EI_1} = \frac{V\beta^3}{bE\alpha^3} \qquad (B.1)$$

The deflection difference of the cracked and un-cracked state is total:

$$\delta = \frac{1.2}{G}\left(\frac{\beta h}{b\alpha h} - \frac{\beta h}{bh}\right) \cdot V + \frac{V\beta^3}{bE\alpha^3} \qquad (B.2)$$

The condition of equilibrium at crack length β is:

$$\partial(V \cdot \delta / 2 - G_c b\beta h) / \partial\beta = 0 \quad \text{or: } \left\{\partial(\delta / V) / \partial\beta\right\} \cdot V^2 / 2 = G_c bh$$

or:

$$V_f = \sqrt{\frac{2G_c bh}{\partial(\delta / V) / \partial\beta}} \qquad (B.3)$$

where G_c is the fracture energy. It follows from eq.(B.2) that:

$$\frac{\partial(\delta / V)}{\partial\beta} = \frac{1.2}{bG}\left(\frac{1}{\alpha} - 1\right) + \frac{3\beta^2}{Eb\alpha^3} \qquad (B.4)$$

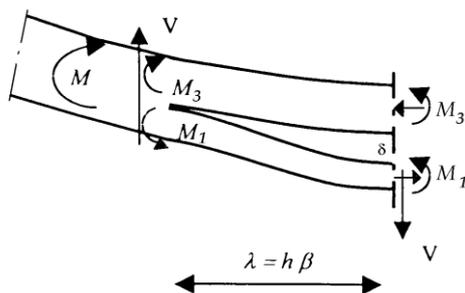Figure B.1. Beam with crack by the dowel force of a joint and bending moment

Figure B.2. Statics of half the crack.

and eq.(B.3) becomes:

$$V_f = b\alpha h \sqrt{\frac{GG_c / h}{0.6(1-\alpha)\alpha + 1.5\beta^2 G / (\alpha E)}} \qquad (B.5) \text{ giving, for the always relatively small}$$

values of *β,* the previous for end-notches found equation: $\dfrac{V_f}{b\alpha h} = \dfrac{\sqrt{GG_c / h}}{\sqrt{0.6 \cdot (1-\alpha) \cdot \alpha}}$

(B.6) which thus also applies for notched beams and for end-joints and verifies the lower bound of the strength, predicted by the theory of [7]. This shows that only work by shear stresses contributes to mode I fracture (elastic shear stress dissipation). This linear elastic fracture mechanics derivation is not enough because design also should be based on "flow " of the joint (embedment flow) at splitting of the beam and the interaction of joint failure and beam splitting has to be regarded. Because plastic flow of the dowel also causes crack opening, the derivation has to be adopted as follows:When crack extension starts of a cantilever beam loaded by a constant load V, giving a deflection increase of δ at V due to this crack extension, then the applied external energy to the beam is $V \cdot \delta$. The energy balance equation then is:

$$V \delta = V \delta / 2 + E_c \tag{B.7}$$

where $V \delta / 2$ is the increase of the elastic energy and E_c the energy of crack extension.

Thus: $E_c = V \delta / 2$ (B.8)

Thus the energy of crack extension is equal to the increase of elastic energy.

Eq.(B.8) also can be written with de incremental deflection $\delta = \mathrm{d}u$:

$$E_c = V^2 \, \mathrm{d}(u/V)/2 = G_f b h \, \mathrm{d}(\beta) \text{ or:}$$

$$V = \sqrt{\frac{2 G_f b h}{\partial (u / V) / \partial \beta}} \tag{B.9}$$

where G_f is the fracture energy per unit crack surface and "$bh\mathrm{d}(\beta)$" the crack surface increase with "b" as width and "h" the height of the beam with a crack length $l = \beta h$.

When the load on the cantilever beam, mentioned above, is prevented to move, the energy balance, eq.(B.7) becomes:

$$0 = E_e + E_c, \text{ or: } E_c = -E_e = -V \delta / 2 \tag{B.10}$$

for the same crack length and now the energy of crack extension is equal to the decrease of elastic energy in the beam.

For a plastic deformation δ of the dowel, there is no elastic deformation and the total external work $V \delta$ is used for plastic dissipation.

When the joint at load V becomes determining and just start to flow at δ_1 when splitting of the beam occurs, (design value of equal strength of joint and beam), then eq.(B.7) becomes:

$$V \delta = (V \delta_1) / 2 + V (\delta - \delta_1) + E_c \tag{B.11}$$

where again $V \delta_1 / 2$ is the increase of the elastic energy and $V (\delta - \delta_1)$ the plastic energy of the flow of the joint. From eq.(B.11) then follows:

$$E_c = V \delta_1 / 2 \tag{B.12}$$

the same as eq.(B.8)..

For dowel connections, plastic deformation is coupled with crack extension. When the dowels of the joint are pressed into the wood, the crack opening occurs and thus also crack extension. Thus for joints is:

$$V \delta = (V \delta_1 - \delta_2) / 2 + V (\delta - \delta_1) + E_s \tag{B.13}$$

where $V \delta_1 / 2$ is the energy of initial crack extension; $V (\delta - \delta_1)$ the plastic energy of embedment flow and $- V \delta_2 / 2$ the decrease of elastic energy due to further crack opening by plastic flow of the dowel, (what takes the whole external applied energy).

From eq.(B.13) now follows:

$$E_s = V (\delta_1 + \delta_2) / 2 \tag{B.14}$$

and eq.(B.9) becomes:

$$V = \sqrt{\frac{2 G_f b h}{\partial ((u_1 + u_2) / V) / \partial \beta}} \tag{B.15}$$

From eq.(B.12) and (B.14) follows that $V_c \delta_{1c} = V (\delta_1 + \delta_2)$, where $V_c \delta_{1c}$ is the amount when the connection is as strong as the beam (according to eq.(B.11). Thus:

$$\frac{\delta_1 + \delta_2}{\delta_{1c}} = \frac{V_c}{V} = \frac{n_c V_n}{n V_n} = \frac{n_c}{n} \tag{B.16}$$

where V_n is the ultimate load of the dowel at flow and n the number of dowels.

Substitution of eq.(B.16) into eq.(B.15) gives:

$$V = \sqrt{\frac{2 G_f b h}{\partial(u_{1c}/V)/\partial\beta} \cdot \frac{n}{n_c}} \quad = b\,\alpha\,h \sqrt{\frac{G\,G_c/h}{0.6(1-\alpha)\alpha + 1.5\beta^2 G/(\alpha E)} \cdot \frac{n}{n_c}} \tag{B.17}$$

what is equal to $\sqrt{n/n_c}$ times the strength according to eq.(B.9) for $u = u_{1c}$, thus $\sqrt{n/n_c}$ times the splitting strength of the beam as is applied in [4].

According to eq.(B.13), the theoretical lower bound of V according to eq.(B.17) occurs at $\delta_1 = \delta_2$, Thus when $n/n_c = 1/2$. In [4], the empirical value of 0.5 to 0.4 is found according to the data of [3] and verified by other known data, giving:

$$V = \sqrt{\frac{2 G_f b h}{\partial(u_{1c}/V)/\partial\beta}} \cdot \sqrt{0,45} = \sqrt{\frac{2 G_f b h}{\partial(u_{1c}/V)/\partial\beta}} \cdot 0.67 \tag{B.18}$$

This Code requirement for "flow" of the joint below failure: $\sqrt{G\,G_f} = 0{,}67 \cdot 18 = 12$ N m m$^{-1.5}$ is included in the Eurocode (see § 7.5 of [4]).

The condition $\delta_1 = \delta_2$ means that there is sufficient elastic energy for total unloading and thus full crack extension with sufficient external work for plastic dissipation by the joints. According to eq.(B.13) is for that case:

$$E_c = V\,\delta_1 \tag{B.19}$$